Electronic Supplementary Material (ESI) for Physical Chemistry Chemical Physics.

The oxygen reduction reaction (ORR) on reduced metals: evidence for a unique relationship between the coverage of adsorbed oxygen species and adsorption energy

*Samuel C. Perry, Guy Denuault**

Chemistry, University of Southampton, Highfield, Southampton, SO17 1BJ, UK.

Supporting Information

Contents

Voltammograms in absence and presence of oxygen

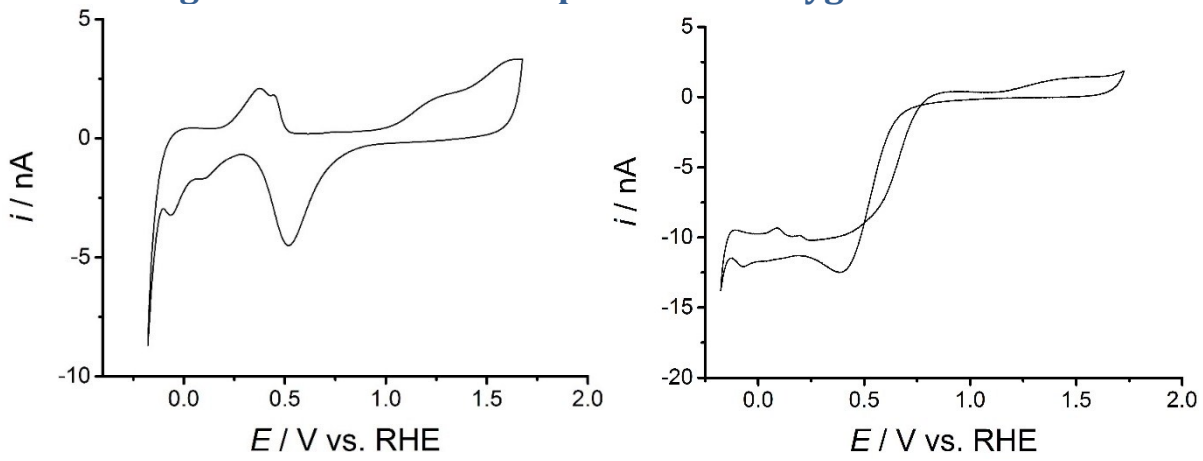

Figure SI-1: Cyclic voltammogram for a 25 µm Ø Pt microdisc recorded in Ar purged (left) and aerated (right) 0.1 M $KClO_4$ at 200 mV s^{-1}.

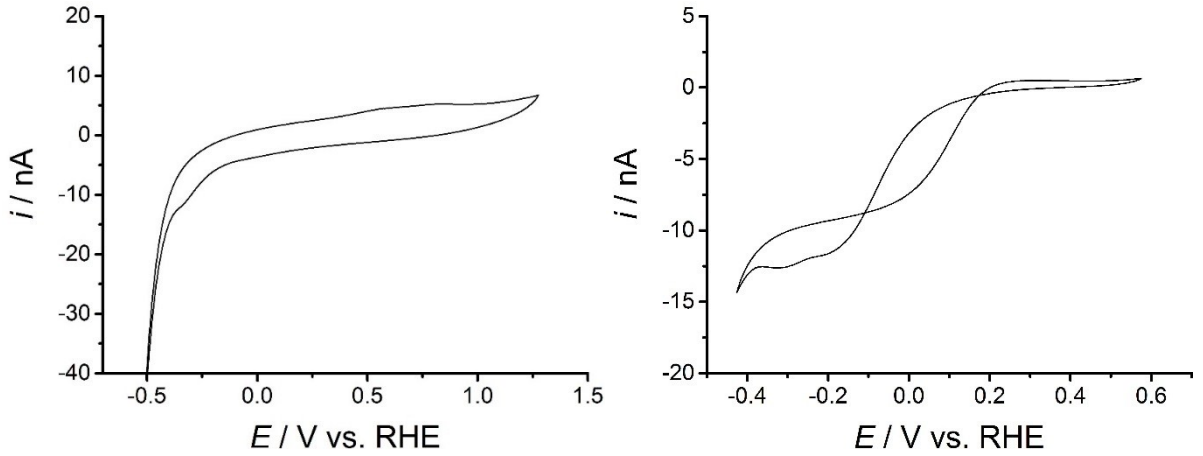

Figure SI-2: Cyclic voltammogram for a 25 µm Ø Ni microdisc recorded in Ar purged (left) and aerated (right) 0.1 M $KClO_4$ at 200 mV s^{-1}.

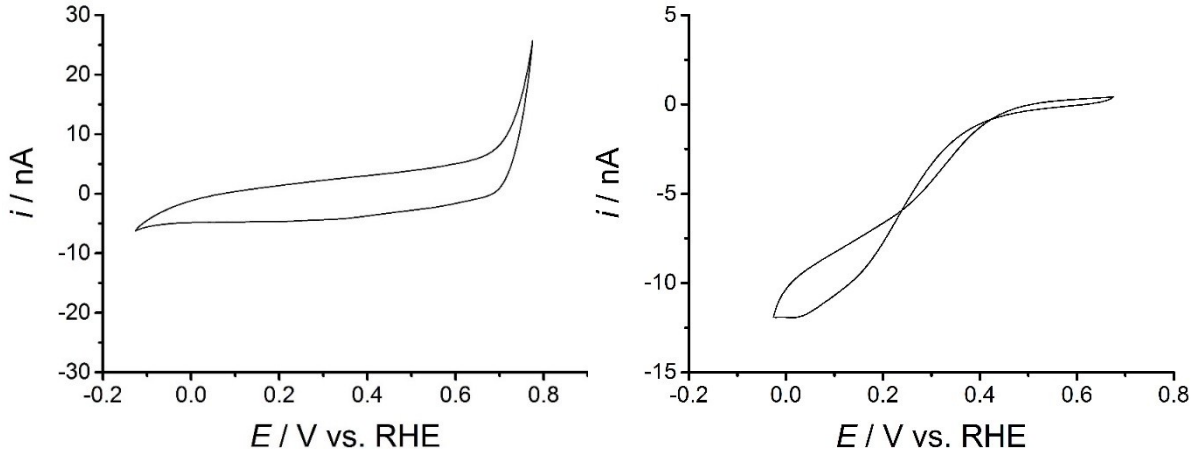

Figure SI-3: Cyclic voltammogram for a 25 µm Ø Cu microdisc recorded in Ar purged (left) and aerated (right) 0.1 M $KClO_4$ at 200 mV s^{-1}.

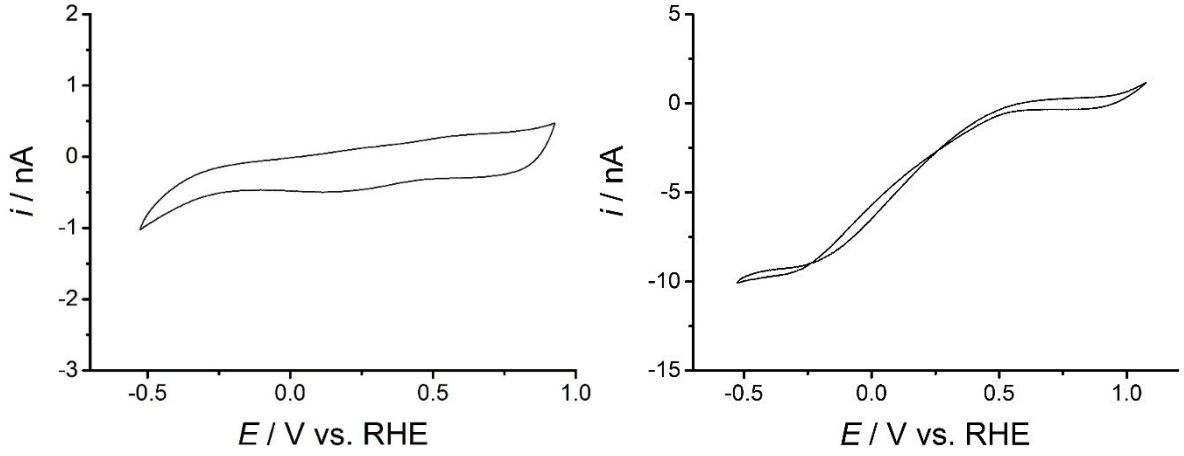

Figure SI-4: Cyclic voltammogram for a 25 µm Ø Ag microdisc recorded in Ar purged (left) and aerated (right) 0.1 M $KClO_4$ at 200 mV s^{-1}.

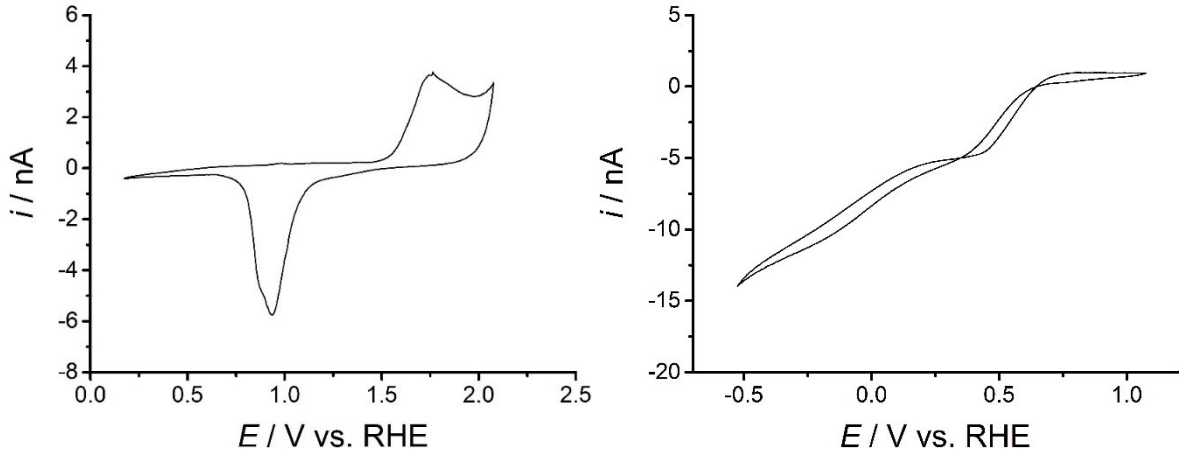

Figure SI-5: Cyclic voltammogram for a 25 µm Ø Au microdisc recorded in Ar purged (left) and aerated (right) 0.1 M $KClO_4$ at 200 mV s^{-1}.

Waveforms for the collection of amperometric data

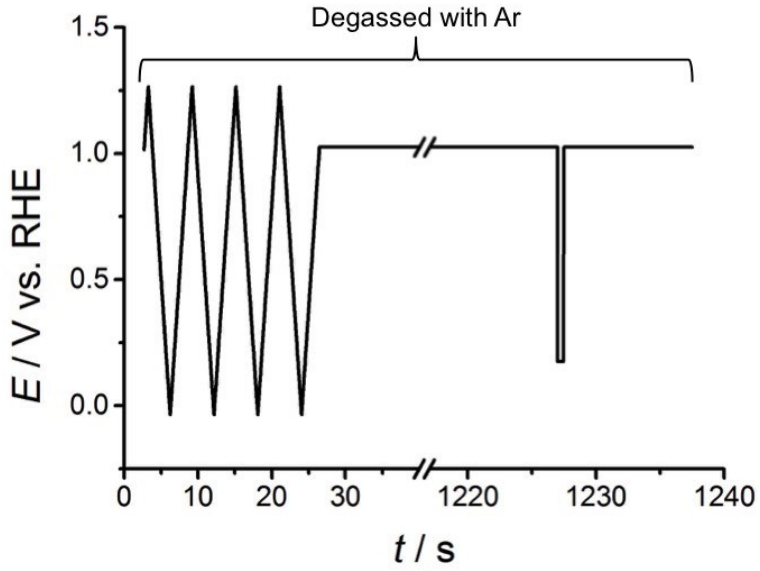

Figure SI-6: Potential waveform used to pre-treat (sweeps) the Pt microdisc and acquire (step) the background chronoamperometric data in Ar purged 0.1 M $KClO_4$.

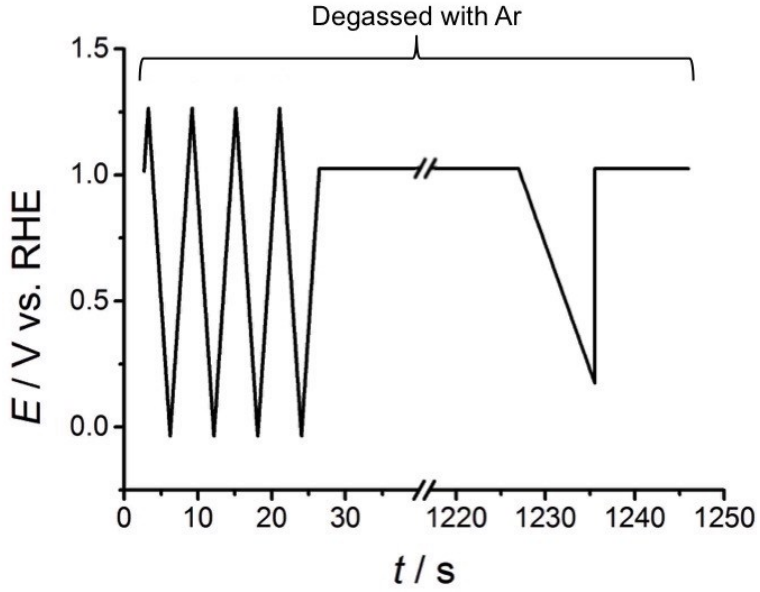

Figure SI-7: Potential waveform used to pre-treat (sweeps) the Pt microdisc and acquire (single sweep) the background LSV in Ar purged 0.1 M $KClO_4$.

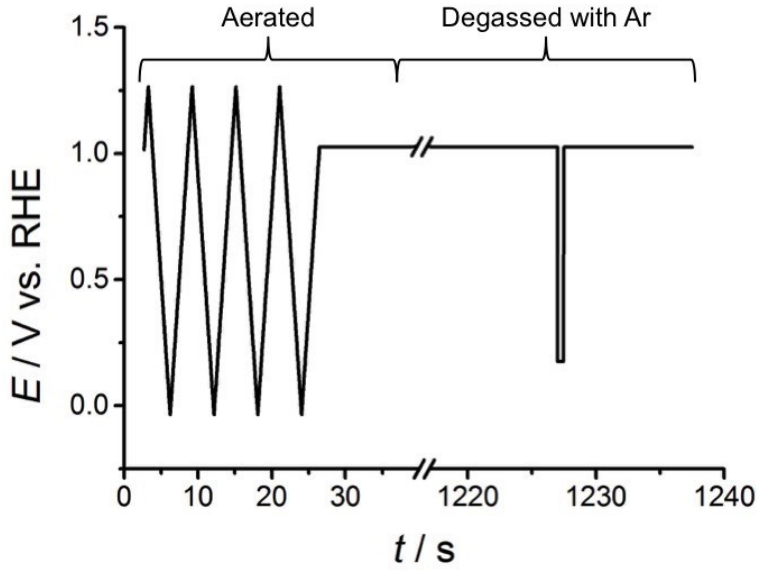

Figure SI-8: Potential waveform used to pre-treat (sweeps) the Pt microdisc and acquire (step) the chronoamperometric data for the reduction of adsorbed oxygen species in 0.1 M $KClO_4$ after removing dissolved oxygen from the solution.

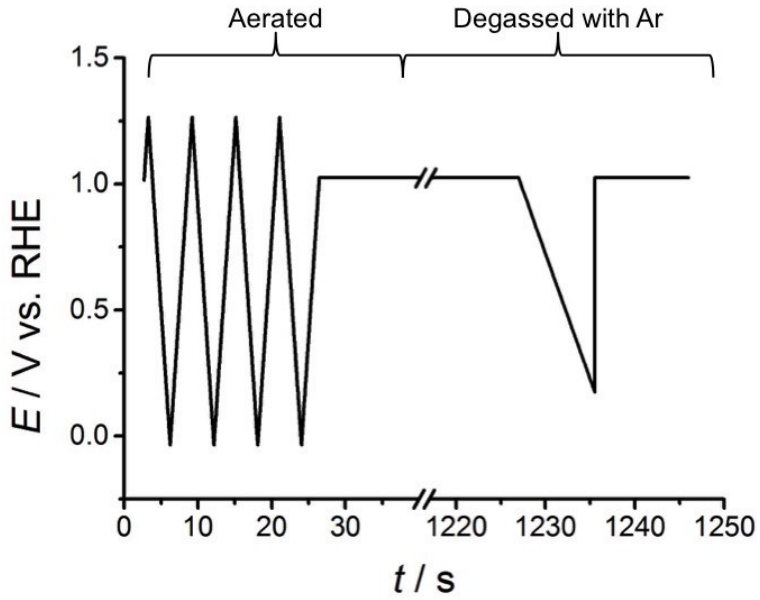

Figure SI-9: Potential waveform used to pre-treat (sweeps) the Pt microdisc and acquire (single sweep) the LSV for the reduction of adsorbed oxygen species in 0.1 M $KClO_4$ after removing dissolved oxygen from the solution.

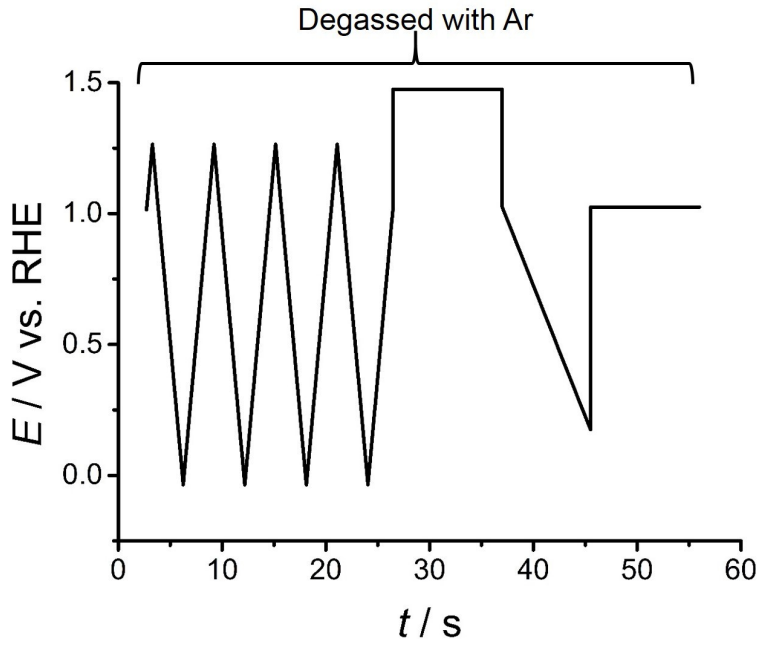

Figure SI-10: Potential waveform used to pre-treat (sweeps) the Pt microdisc and acquire (single sweep) the LSV for the reduction of oxide species in 0.1 M $KClO_4$.

Waveform potentials for all metals

Table SI-1: Potentials used for the upper and lower cleaning potentials, stepped potential, and rest potential for the waveform shown in Figure SI-8.

	Potentials / V vs. RHE			
Metal	**Rest Potential**	**Upper Cleaning Potential**	**Lower Cleaning Potential**	**Stepped Potential**
Au	0.60	0.85	-0.35	-0.25
Ag	0.70	0.95	-0.15	0.05
Pt	1.00	1.25	-0.05	0.15
$Pt_{0.9}Rh_{0.1}$	1.00	1.25	-0.05	0.15
$Pt_{0.9}Ir_{0.1}$	1.00	1.25	-0.05	0.15
Cu	0.60	0.75	-0.15	-0.05
Ni	0.35	0.85	-0.55	-0.45

Chronoamperograms and Cottrell plots for all microelectrodes

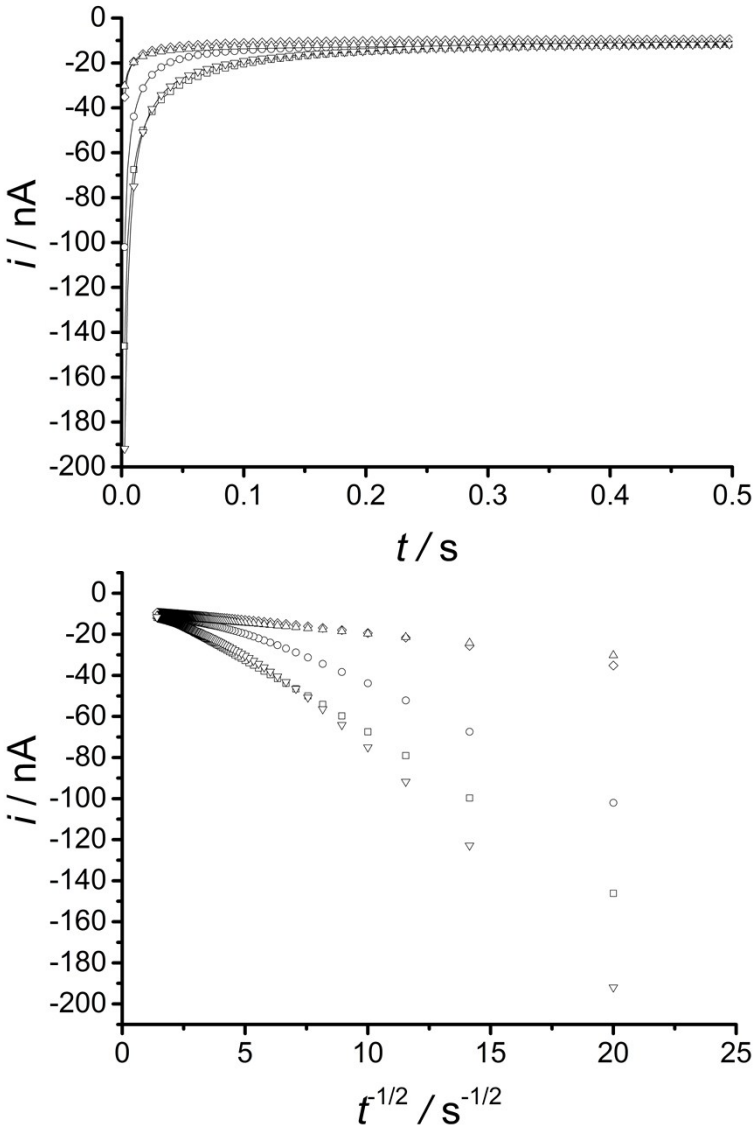

Figure SI-11: Chronoamperograms (top) and corresponding Cottrell plots (bottom) for the reduction of oxygen in aerated 0.1 M $KClO_4$ with a 25 µm Ø Au (△), Ag (◇), Pt (○), Cu (□)and Ni (▽) electrode. Each electrode was conditioned as shown above.

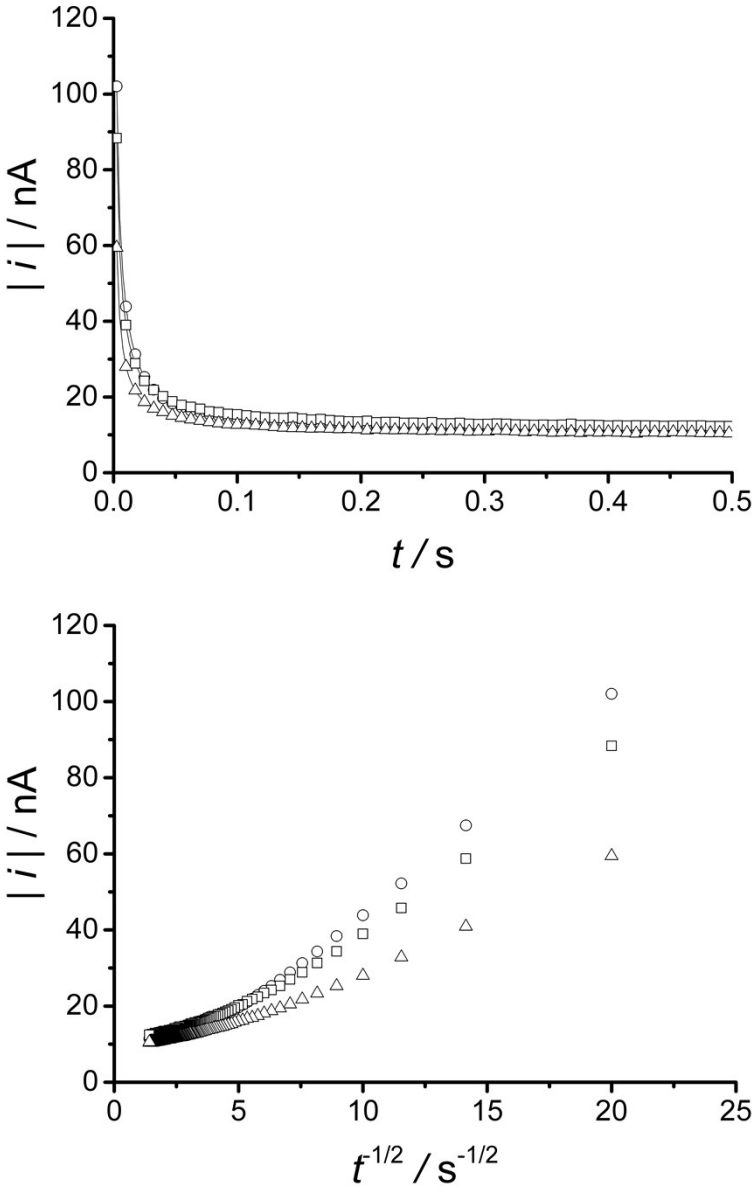

Figure SI-12: Chronoamperograms (top) and corresponding Cottrell plots (bottom) for the reduction of oxygen in aerated 0.1 M $KClO_4$ with a 25 µm Ø Pt (○), $Pt_{0.9}Ir_{0.1}$ (Δ) and $Pt_{0.9}Rh_{0.1}$ (□) electrode. Each electrode was conditioned as shown above.

Estimation of the adsorption energies from the voltammograms

The adsorption energy of the oxygen species, $^{\Delta G_{peak}}$, was derived from the difference between ^{E_p}, the potential at which the adsorbed oxygen species are stripped, and $^{E_{ORR}}$, the potential at which the oxygen molecule should be reduced in absence of kinetic limitations, i.e. the thermodynamic potential for oxygen reduction.

$$\Delta G_{peak} = -nF(E_{ORR} - E_p) \quad (1)$$

$^{E_{ORR}}$ was calculated by adjusting the thermodynamic potential for oxygen reduction, 1.229 V vs. SHE, for the measured pH. For pH 7.34, $^{E_{ORR}} =$ 0.796 V vs. RHE.

$$E_{ORR} = 1.229\ V - 0.059\ \times pH \quad (2)$$

ΔG_{peak} was calculated in this way for all metals taking n as two electrons per oxygen atom because the extra charge is determined from chronoamperometric transients recorded at large overpotentials where complete reduction of oxygen should be observed irrespective of the metal.

Estimation of the electrode electroactive area

For Pt the electroactive area, A, was found from the charge under the hydride adsorption region of a 20 mV s^{-1} CV in 1 M H_2SO_4,

$$A = \frac{0.77}{210\ \mu C\ cm^{-2}} \int_{0.02\ V\ vs.\ RHE}^{0.35\ V\ vs.\ RHE} i\ dt \tag{3}$$

where integrating the current between the double layer region and the trough in the hydride adsorption region prior to hydrogen evolution for the acid CV gives 0.77 monolayers of hydride and a single monolayer of hydride corresponds to 210 µC cm^{-2} of charge[1].

This method was only possible for the platinum electrode thanks to its well defined and well-studied hydrogen adsorption region. For the other metal electrodes, the electroactive area was calculated by multiplying their geometric area by the roughness factor of the platinum electrode (R_f), which is taken as the ratio between the electrode electroactive surface area and its geometric area. After undergoing a standard polishing regime, the R_f was found to be 2.6. As all electrodes underwent the same polishing regime, it is a reasonable assumption that they will exhibit the same roughness factor.

Estimation of the oxygen coverage

This was done by first calculating the number of moles of dioxygen that would make up a complete monolayer (N_{O_2}) from

$$N_{O_2} = \frac{A\ N_{Pt,\ cm^{-2}}}{2N_A} \tag{4}$$

where $N_{Pt,\ cm^{-2}}$=1.3×10^{15} cm^{-2} is the average number of Pt surface atoms found in polycrystalline platinum,[2] N_A is Avogadro's number and A is the electroactive surface area of the electrode. The factor of two arises from the assumption that each Pt atom binds to one oxygen atom. For a 25 µm Pt microdisc electrode, the number of adsorption sites for O_2 was found to be 3.68×10^9, which equates to 6.11×10^{-15} mol in a complete monolayer. The number of moles of oxygen actually present on the electrode surface was found from the extra charge passed using Faraday's law of electrolysis assuming a 4 electron reduction. For the direct reduction of the adsorbed oxygen (experiments done with waveform shown in figure SI-8), Q_{ads} corresponds to 1.5×10^{-15} mol of adsorbed dioxygen. For the extra charge seen in fully aerated solution, Q_{extra} corresponds to 1.9×10^{-15} mol. These values respectively correspond to 0.08 and 0.10 monolayers of adsorbed dioxygen.

A similar approach was followed to estimate the dioxygen coverage on the other metals, except that the number of metal atoms was taken as 1.2×10^{15}, 1.0×10^{15}, 1.8×10^{15}, 1.6×10^{15} cm^{-2}, for Au, Ag, Cu and Ni surfaces respectively.[3-6] For simplicity we assumed that the Pt alloys had the same number of atoms per unit area as Pt.

ORR kinetic currents

For each microdisc the kinetically controlled ORR current, i_k, was estimated with equation 5 from the experimental current measured at 0.45 V vs RHE, i_{exp}, on sampled current voltammograms (SCV) recorded in aerated 0.1 M $KClO_4$ as previously reported.[7] To ensure the current was not affected by iR drop the SCV were constructed from current transients sampled at 500 ms. At 0.45 V i_{exp} corresponds to 50 % of the diffusion controlled current, i_d, as recommended by Vidal-Iglesias et al.[8]

$$i_k = \frac{i_d i_{exp}}{i_d - i_{exp}} \tag{5}$$

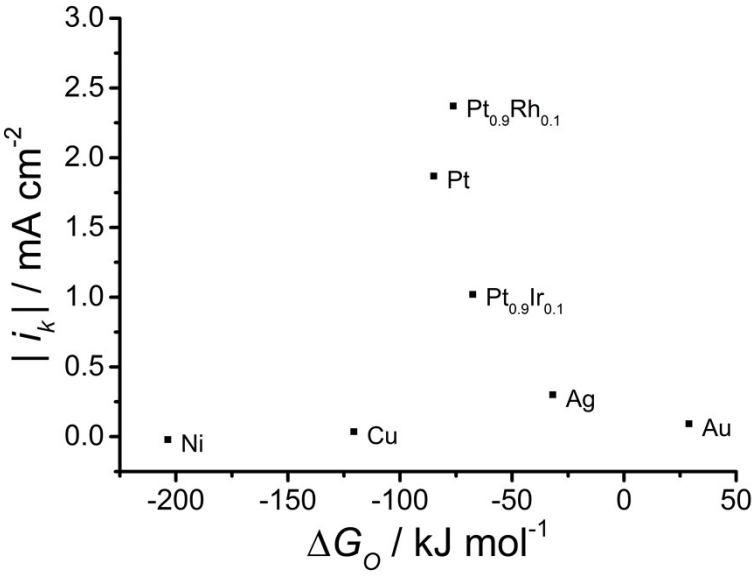

Figure SI-13: Experimental ORR kinetic currents measured at 0.45 V vs RHE with the different microdisc electrodes plotted versus the theoretical adsorption energies taken from ref.[9] This is the blue curve shown on the 3D plot in Figure 6.

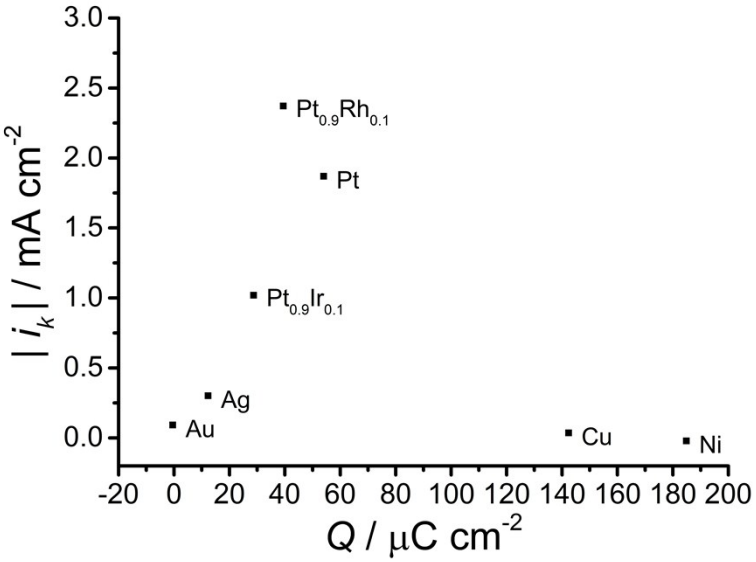

Figure SI-14: Experimental ORR kinetic currents measured at 0.45 V vs RHE with the different microdisc electrodes plotted versus the experimental charge for the reduction of the adsorbed oxygen species. This is the green curve shown on the 3D plot in Figure 6.

References

1. T. Biegler, D. A. J. Rand and R. Woods, *J. Electroanal. Chem.*, 1971, **29**, 269-277.
2. S. H. Sun, G. X. Zhang, D. S. Geng, Y. G. Chen, R. Y. Li, M. Cai and X. L. Sun, *Angew. Chem. Int. Ed.*, 2011, **50**, 422-426.
3. S. Mullegger, O. Stranik, E. Zojer and A. Winkler, *Applied Surface Science*, 2004, **221**, 184-196.
4. S. Prusa, P. Prochazka, P. Babor, T. Sikola, R. ter Veen, M. Fartmann, T. Grehl, P. Bruner, D. Roth, P. Bauer and H. H. Brongersma, *Langmuir*, 2015, **31**, 9628-9635.
5. M. Pedio, C. Cepek and R. Felici, in *Noble Metals*, ed. Y.-H. S. (Ed.), InTech, 2012, DOI: 10.5772/34551, ch. 12, pp. 249-286.
6. J. W. Geus, in *Hydrogen Effects in Catalysis: Fundamentals and Practical Applications (Chemical Industries)*, eds. Z. Paál and P. G. Menon, Marcel Dekker, Inc., 1988.
7. S. C. Perry and G. Denuault, *Physical chemistry chemical physics : PCCP*, 2015, **17**, 30005-30012.
8. F. J. Vidal-Iglesias, J. Solla-Gullon, V. Montiel and A. Aldaz, *Electrochem. Commun.*, 2012, **15**, 42-45.
9. J. K. Norskov, J. Rossmeisl, A. Logadottir, L. Lindqvist, J. R. Kitchin, T. Bligaard and H. Jonsson, *J. Phys. Chem. B*, 2004, **108**, 17886-17892.